Available online at www.sciencedirect.com

ScienceDirect

Spectrochimica Acta Part A 66 (2007) 250–261

SPECTROCHIMICA ACTA PART A

www.elsevier.com/locate/saa

Structure and spectroscopic characteristics of 4-*tert*-butylphenoxyacetylhydrazones of arylaldehydes

S.N. Podyachev [a,*], I.A. Litvinov [a], R.R. Shagidullin [a], B.I. Buzykin [a], I. Bauer [b], D.V. Osyanina [a], L.V. Avvakumova [a], S.N. Sudakova [a], W.D. Habicher [b], A.I. Konovalov [a]

[a] *A.E. Arbuzov Institute of Organic and Physical Chemistry, Kazan Scientific Center of Russian Academy of Sciences, Arbuzov str. 8, 420088 Kazan, Russia*
[b] *Dresden University of Technology, Institute of Organic Chemistry, Mommsenstraße 13, D-01062 Dresden, Germany*

Received 15 December 2005; received in revised form 22 February 2006; accepted 22 February 2006

Abstract

By reaction of 4-*tert*-butylphenoxyacetylhydrazide with aromatic aldehydes and acetone a new series of 4-*tert*-butylphenoxyacetylhydrazones was synthesized. The structural peculiarities of the investigated molecules have been determined by means of X-ray analysis and IR spectroscopy. The diagnostically important IR spectral criteria required for the conformational analysis of acethylhydrazones have been considered. It was established that the 4-*tert*-butylphenoxyacetylhydrazide in condensed phase exists only as a $\mathbf{Z}_{\text{N–C(O)}}$-conformer. Its derivatives exist as $\mathbf{E}_{\text{N–C(O)}}$ and $\mathbf{Z}_{\text{N–C(O)}}$-forms. As a rule, the prevalence of $\mathbf{Z}_{\text{N–C(O)}}$-form has been observed in CCl_4 solutions. The structure of investigated compounds is also determined by a system of inter- and intramolecular hydrogen bonds. The energy of hydrogen bonds was estimated.

Keywords: 4-*tert*-Butylphenoxyacetylhydrazide; 4-*tert*-Butylphenoxyacetylhydrazones; Conformation; Hydrogen bonds; IR spectroscopy; X-ray crystallography

1. Introduction

Hydrazides and acylhydrazones are nowadays of considerable technical and commercial importance [1]. This is connected with their wide using as drugs, complexones, photothermochromic compounds and precursors for organic synthesis [2–4]. In case of acylhydrazones the presence of the carbonyl oxygen atom promotes the formation of a chelate binding center [3]. It also leads to the formation of $\mathbf{E}_{\text{N–C(O)}}/\mathbf{Z}_{\text{N–C(O)}}$ amide conformers (Scheme 1) due to the hindered rotation around the N–C(=O) bond [5,6].

The influence of functional groups in acetylhydrazone fragment of molecules and the character of hydrogen bonds on the configuration equilibrium in hydrazones is insufficiently investigated. Taking this fact into consideration, we investigated the structure of 4-*tert*-butylphenoxyacetylhydrazyde and its condensation products with carbonyl compounds (Scheme 2). The peculiarity of these compounds is the presence of an ether oxygen atom and conformationally labile C–C and C–O bonds. This increases the probability of the realization of a large number of conformers and the formation of additional hydrogen bonds. These compounds are also of interest as structural blocks of calix[4]arene derivatives [7,8].

In this paper we show IR spectroscopy data of 4-*tert*-butylphenoxyacetylhydrazide and 4-*tert*-butylphenoxyacetylhydrazones of arylaldehydes in solid state and in non-polar solvent (CCl_4) along with the results of the single crystal X-ray diffraction study.

2. Experimental

2.1. Materials

All reagents were used as commercially received without further purification. K_2CO_3 (p.a.) was annealed prior to use. The general synthetic methods and the structure formulae of the investigated compounds are presented in Scheme 2. The ethyl ester of 4-*tert*-butylphenoxyacetic acid (**1**) and 4-*tert*-butylphenoxyacetylhydrazide (**2**) used in this work were obtained according to literature methods [9,10]. The composition and the structure of the obtained compounds have been confirmed by means of elemental analysis, ^{1}H NMR (Table 1), IR spectroscopy and X-ray analysis. The purity of the compounds was monitored by TLC.

---

[*] Corresponding author. Tel.: +7 843 2727394; fax: +7 843 2732253.
E-mail address: spodyachev@iopc.knc.ru (S.N. Podyachev).

1386-1425/$ – see front matter © 2006 Elsevier B.V. All rights reserved.
doi:10.1016/j.saa.2006.02.049

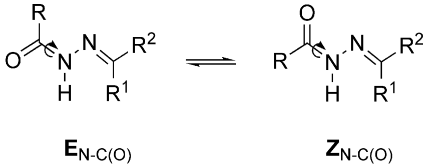

Scheme 1.

2.1.1. Preparation of the 4-tert-butylphenoxyacetylhydrazone of acetone (3)

A solution of (3 mmol) 4-*tert*-butylphenoxyacetylhydrazide (**2**) in 5 ml water and 10 ml acetone was refluxed for 3 h. The precipitate was filtered off and washed several times with distilled water. **3** (0.65 g, 82%) was obtained as a white powder (mp 70–72 °C; elemental analysis for $C_{15}H_{22}N_2O_2$, calculated: C, 68.67; H, 8.45; N, 10.68%; found: C, 68.70; H, 8.67; N, 10.98%).

2.1.2. General procedure for the synthesis of 4-tert-butylphenoxyacetylhydrazones of aromatic aldehydes (4–9)

To a boiling solution of (3 mmol) 4-*tert*-butylphenoxyacetylhydrazide (**2**) in 4 ml EtOH under stirring were added 3 mmol of the corresponding aldehyde (4-bromobenzaldehyde and 4-nitrobenzaldehyde were initially dissolved in 3 ml hot EtOH). The reaction mixture was refluxed for 1 h. In the case of compounds **4–7** the precipitate was filtered off, washed several times with a mixture of water/EtOH (1:1), and recrystallized from EtOH. As a result of the synthesis of compounds **8** and **9** no precipitate was formed. The solvent was removed from the reaction mixture by distillation and the solid remainder was washed with hexane and recrystallized from CCl_4.

2.1.2.1. 4-tert-Butylphenoxyacetylhydrazone of benzaldehyde (4). **4** (0.84 g, 90%) was obtained as a white powder (mp 172 °C; elemental analysis for $C_{19}H_{22}N_2O_2$, calculated: C, 73.52; H, 7.14; N, 9.03%; found: C, 73.38; H, 8.07; N, 9.51%).

2.1.2.2. 4-tert-Butylphenoxyacetylhydrazone of 4-bromobenzaldehyde (5). **5** (1.1 g, 93%) was obtained as a white powder (mp 155–157 °C; elemental analysis for $C_{19}H_{21}Br_1N_2O_2$, calculated: C, 58.62; H, 5.44; N, 7.20; Br, 20.53%; found: C, 58.63; H, 5.77; N, 7.27; Br, 21.13%).

2.1.2.3. 4-tert-Butylphenoxyacetylhydrazone of 4-nitrobenzaldehyde (6). **6** (0.63 g, 59%) was obtained as a yellowish powder (mp 184 °C; elemental analysis for $C_{19}H_{21}N_3O_4$, calculated: C, 64.21; H, 5.96; N, 11.82%; found: C, 64.52; H, 5.74; N, 12.18%).

2.1.2.4. 4-tert-Butylphenoxyacetylhydrazone of salicylaldehyde (7). **7** (0.92 g, 90%) was obtained as a white powder (mp 165–167 °C; elemental analysis for $C_{19}H_{22}N_2O_3$, calculated: C, 69.92; H, 6.79; N, 8.58%; found: C, 69.97; H, 7.80; N, 9.13%).

2.1.2.5. 4-tert-Butylphenoxyacetylhydrazone of pyridine-4-carbaldehyde (8). **8** (0.72 g, 77%) was obtained as a white powder (mp 93 °C; elemental analysis for $C_{18}H_{21}N_3O_2$, cal-

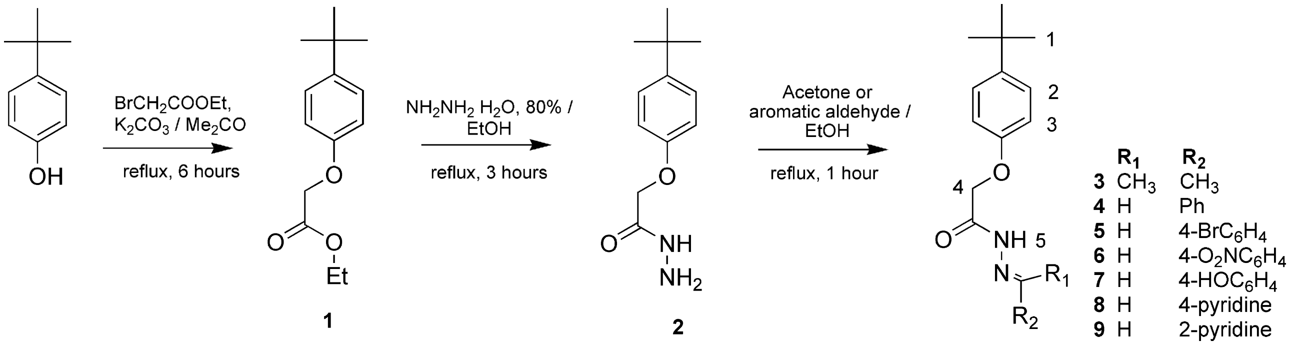

Scheme 2.

Table 1

^{1}H chemical shifts[a] (ppm) of $\mathbf{Z}_{N\text{–}C(O)}$ ($\mathbf{E}_{N\text{–}C(O)}$)-conformers **3–9** in $CDCl_3$

Compound	H-1	H-2[b]	H-3[b]	H-4	H-5	R$_1$	R$_2$
3	1.29 (1.28)	7.34 (7.29)	6.87 (6.90)	4.61 (4.98)	9.10 (8.39)	2.12 (2.02)	1.89 (1.84)
4	1.32 (1.30)	7.36 (7.32)	6.92 (6.96)	4.67 (5.16)	9.55 (10.08)	8.25 (7.86)	7.38–7.77[c]
5	1.31 (1.30)	7.36 (7.32)	6.91 (6.94)	4.67 (5.14)	9.99 (9.55)	8.21 (7.79)	7.54–7.64[c]
6	1.31 (1.26)	7.36 (7.32)	6.91 (6.94)	4.68 (5.17)	9.75 (10.35)	8.44 (7.97)	7.79–8.26[c]
7	1.30 (1.27)	7.34 (7.23)	6.89 (6.92)	4.64 (4.98)	10.91 (9.90)	8.43 (7.97)	6.99–7.20[c]; 9.52[d] (9.97[d])
8	1.31 (1.28)	7.36 (7.32)	6.91 (6.94)	4.68 (5.16)	9.75 (10.35)	8.35 (7.83)	7.49–8.68[c]
9	1.31 (1.29)	7.35 (7.29)	6.91 (6.94)	4.69 (5.15)	9.68 (9.29)	8.28 (7.96)	7.28–8.16[c]

[a] Numbering follows from Scheme 2.

[b] Doublet ($^3J \approx 8.6$ Hz).

[c] Chemical shifts for conformers are not assigned due to signals overlapping.

[d] OH proton.

culated: C, 69.43; H, 6.80; N, 13.49%; found: C, 67.96; H, 7.00; N, 13.88%).

2.1.2.6. 4-tert-Butylphenoxyacetylhydrazone of pyridine-2-carbaldehyde (9). **9** (0.74 g, 79%) was obtained as a white powder (mp 119–121 °C; elemental analysis for $C_{18}H_{21}N_3O_2$, calculated: C, 69.43; H, 6.80; N, 13.49%; found: C, 70.41; H, 7.56; N, 14.10%).

2.2. Spectroscopy

Microanalyses of C, H, N were carried out with a CHN-S analyser (Carlo Erba). ^{1}H NMR spectra were recorded on a Bruker MSL-400 instrument with a working frequency of 400.13 MHz. Chemical shifts in δ have been determined in $CDCl_3$ with Me_4Si as an internal standard at a temperature of 30 °C. The signals for conformers were assigned in accordance with [5,6]. IR absorption spectra of Nujol emulsions and CCl_4 solutions (10^{-2} to 10^{-5} M) of compounds were recorded on a Vector-22 Bruker FT-IR spectrophotometer with a resolution of 4 cm^{-1}.

2.3. Crystal structure determination

The X-ray diffraction data were collected on a CAD-4 Enraf-Nonius automatic diffractometer using graphite monochromated Cu Kα (λ = 1.54184 Å) radiation. The details of crystal data, data collection and the refinement are given in Table 2. The stability of crystals and experimental conditions were being checked every 2 h using three control reflections, while the orientation was being monitored every 200 reflections by centering two standards. No significant decay was observed. Corrections for Lorentz and polarization effects were applied. Absorption correction was not applied. The structures **2**, **7** were solved by direct methods using MolEN package [11], and structures **4**, **6** were solved and refined by direct methods using SHELX-97 package [12]. For the crystals all non-hydrogen atoms were refined anisotropically. H-atoms, located in ΔF maps, were included into structure factor calculations with fixed positional and thermal parameters in structures **2**, **7** and refined as riding atoms. All figures were made using the program PLATON [13]. Crystals **4** and **7** are isostructural, so for **4** the figures have not been represented. All crystallographic data (excluding structure factors) for the structures are deposited with the Cambridge Crystallographic Data Centre (deposition number CCDC 271697-271700).

3. Results

3.1. X-ray analysis

According to the X-ray data hydrazide **2** exists in the crystal phase only as a $\mathbf{Z}_{\mathrm{N-C(O)}}$-conformer (Fig. 1, **2**). This conformation is stabilized by intramolecular hydrogen bonds between the amide hydrogen atom and the oxygen atom of the phenoxy groups (Fig. 2, **2**) As a result the phenyl ring (plain P1) and the plain P2, which includes the hydrazide fragment and OCH_2-bridge, are practically coplanar (Table 3).

The hydrogen atom of the amide group in hydrazide **2**, additionally to its involvement in the intramolecular hydrogen bond, at the same time takes part in the formation of an intermolecular hydrogen bond with the C=O group of the neighbouring molecule (see Fig. 2, **2**). One of the hydrogen atoms of the terminal amino group of hydrazide **2** is also involved in the formation of intermolecular H-bonds with the carbonyl oxygen of another molecule ($1/2+x$, $3/2-y$, z), which leads to a non-equivalence of the protons of the primary amino group.

The parameters of the H-bonds are the following: intramolecular—N(1)–H(1)···O(2), N(1)–H(1) 1.15 Å, H(1)···O(2) 1.89 Å, N(1)···O(2) 2.607(4) Å, angle N(1)–H(1)···O(2) 117°; intermolecular—N(1)–H(1)···O(1′) [$3/2-x$, $-1/2+y$, $-z$], H(1) ···O(1′) 2.26 Å, N(1)···O(1′) 3.219(4) Å, angle N(1)–H(1)···O(1′) 140°; N(2)–H(201)···O(1″) [$1/2+x$, $3/2-y$, z], N(2)–H(201) 1.20 Å, H(201)···O(1″) 1.89 Å, N(2)···O(1″) 3.078(3) Å, angle N(2)–H(201)···O(1″) 170°. The system of hydrogen bonds in the crystal of hydrazide **2** represents a flattened two-dimensional network parallel to the plain XOZ (Fig. 2, **2**).

In the crystal of hydrazone **4** the asymmetric part of the unit cell contains two independent molecules (**4A** and **4B**), wherein the *tert*-butyl group of molecule **4B** is disordered. The main geometric parameters (bond lengths and bond angles) in the two independent molecules are the same within the limits of experimental error (excluding the disordered *tert*-butyl group, for which the geometric parameters have been determined with low accuracy). The non-hydrogen atoms of the carbonylhydrazone and the oxymethyl groups are practically in one plain P2 (see Table 3). This plane has a dihedral angle only of 8.1° (molecule **4A**) and 10.2° (molecule **4B**) with the phenyl ring (plain P3) of the benzylidene fragment. In contrast to hydrazide **2**, in this case the **Z**-conformer takes place relative to the bond C(1)–C(2), however, the *tert*-butylphenoxy moiety is rotated around the C(2)–O(2) bond by −77.4(2)° and 81.3(2)°, respectively, in molecules **4A** and **4B**. Thus, apart from minor differences in the size of torsion angles and the direction of the torsion of substituents in respect of the C(2)–O(2)-bonds, the geometry of the molecules **4A** and **4B** is similar.

The independent molecules **4A** and **4B** in the crystal of hydrazone **4** form cyclic dimers of the type **4A**···**4B′** (or **4A′**···**4B**) due to N–H···O hydrogen bonds (Fig. 2, **7**). The parameters of the hydrogen bonds are the following: N(1A)–H(1A)···O(1B′) [$1+x$, y, $z-1$], N(1A)–H(1A) 0.92 Å, H(1A)···O(1B′) 1.96 Å, N(1A)···O(1B′) 2.874(4) Å, angle N(1A)–H(1A)···O(1B′) 173°; N(1B)–H(1B)···O(1A″) [$x-1$, y, $1+z$], N(1B)–H(1B) 0.86 Å, H(1B)···O(1A) 2.03 Å, N(1B)···O(1A″) 2.887(4) Å, angle N(1B)–H(1B)···O(1A″) 172°.

The crystals of hydrazone **7** are isostructural to the crystals of hydrazone **4** (see Table 2). However the disorder of *tert*-butyl substituents in molecules **7** is not observed (Fig. 1, **7**). The presence of *ortho*-hydroxy groups in the phenyl ring of hydrazone **7** does not lead to a change in the crystal packing. The conformation of the independent molecules **7** is also similar to the

Table 2
Single-crystal X-ray data for structures **2**, **4**, **6** and **7**

Parameter	**2**	**4**	**6**	7
Chemical formula	$C_{12}H_{18}N_2O_2$	$C_{19}H_{22}N_2O_2$	$C_{19}H_{21}N_3O_4$	$C_{19}H_{22}N_2O_3$
Color, shape	Colorless, prismatic	Colorless, prismatic	Light yellow prismatic	Colorless prismatic
Lattice type	Monoclinic	Triclinic	Monoclinic	triclinic
Space group	*P*2$_1$/*a*	*P*-1	*Pa*	*P*-1
Cell dimensions	$a = 8.154(4)$ Å $b = 9.55(1)$ Å $c = 16.68(1)$ Å $\beta = 91.86(4)°$	$a = 9.175(6)$ Å $b = 12.37(1)$ Å $c = 16.88(1)$ Å $\alpha = 89.90(6)°$ $\beta = 75.25(6)°$ $\gamma = 72.85(6)°$	$a = 10.55(1)$ Å $b = 6.362(3)$ Å $c = 14.389(9)$ Å $\beta = 108.51(9)°$	$a = 8.967(9)$ Å $b = 12.67(1)$ Å $c = 16.71(2)$ Å $\alpha = 89.39(9)°$ $\beta = 75.72(8)°$ $\gamma = 74.25(8)°$
Volume (Å^3)	1298 (2)	1765 (3)	915 (2)	1768 (3)
Z	4	4 (two independent molecules)	2	4 (two independent molecules)
Formula weight	222.29	310.40	355.40	326.40
Calculated density (g/cm^3)	1.137	1.168	1.290	1.226
μ (Cu Kα) (mm^{-1})	0.598	0.574	0.717	0.639
F(0 0 0)	480	664	376	696
Radiation, λ (Å)	Cu Kα, λ = 1.54184 Å			
θ, Measurement interval (°)	2.72–74.22	2.72–57.23	6.96–65.00	2.72–74.22
Scan angle	ω			
Reflections limits	$-10 \le h \le 10$ $0 \le k \le 11$ $0 \le l \le 20$	$-10 \le h \le 8$ $-13 \le k \le 13$ $-18 \le l \le 0$	$-12 \le h \le 11$ $0 \le k \le 7$ $0 \le l \le 16$	$-11 \le h \le 10$ $-15 \le k \le 15$ $-20 \le l \le 0$
Total reflections measured	2910	4739	1675	6984
Reflections with $F^2 > 2\sigma$(I)	1392 [>3σ(I)]	3903	1583	3555 [>3σ(I)]
Number of parameters	145	452	272	433
Absorption correction	Not applied			
Hydrogen treatment	Included not refined	Mixed	Mixed	Included not refined
Final *R*-factors [$F^2 > 2\sigma$(I)]	$R1 = 0.065$ w$R2 = 0.077$	$R1 = 0.054$ w$R2 = 0.161$	$R1 = 0.051$ w$R2 = 0.127$	$R1 = 0.055$ w$R2 = 0.065$
Goodness of fit on F^2	2.275	1.027	1.103	1.936

conformation of the molecules **4**. The main geometric parameters of molecules **4** correspond to those of molecules **7** within the limits of experimental errors.

The analysis of intra- and intermolecular interactions in crystal **7** showed that the hydroxyl group forms an intramolecular H-bond with the imine nitrogen atom. Similar as in crystal **4** intermolecular hydrogen bonds bind molecules **7A** and **7B** in the dimers (Fig. 2, **7**).

The parameters of the hydrogen bonds are the following: O(15A)–H(15A)···N(2A), O(15A)–H(15A) 1.22(3) Å, H(15A)···N(2A) 1.59(3) Å, O(15A)···N(2A) 2.633(4) Å, angle O(15A)–H(15A)···N(2A) 138(2)°; O(15B)–H(15B)···N(2B), O(15B)–H(15B) 1.13(3) Å, H(15B)···N(2B) 1.74(3) Å, O(15B)···N(2B) 2.643(4) Å, angle O(15B)–H(15B)···N(2B) 133(2)°; N(1A)–H(1A)···O(1B′) [$-x$, $2-y$, $1-z$], N(1A)–H(1A) 1.15(2) Å, H1A···O1B′ 1.69(2) Å, N(1A)···O(1B′) 2.820(3) Å, angle N(1A)–H(1A)···O(1B′) 169(2)°; N(1B)–H(1B)···O(1A″) [$-x$, $1-y$, $1-z$], N(1B)–H(1B) 1.16(3), H(1B)···O(1A″) 1.72(3) Å, N(1B)···O(1A″) 2.876(3) Å, angle N(1B)–H(1B)···O(1A″) 175(2)°.

Table 3
Dihedral angles (°) between planes P1(C3–C4–C5–C6–C7–C8), P2(O2–C2–C1–O1–N1–N2–C13)[a] and P3(C14–C15–C16–C17–C18–C19) for the structures **2**, **4**, **6** and **7**

Molecule	P1/P2	P1/P3	P2/P3
2	5.7 (8)	–	–
4a	80.99 (9)	73.61 (8)	8.1 (6)
4b	83.43 (8)	85.29 (8)	10.2 (4)
6	35.5 (2)	13.8 (7)	21.7 (3)
7a	80.96 (8)	76.25 (9)	5.3 (9)
7b	84.87 (8)	83.24 (9)	11.2 (4)

[a] For compound **2** plane P2 (O2–C2–C1–O1–N1–N2).

In molecule **6** hydrazone and amide fragments are located in one plain P2 as in molecules mentioned above. However the introduction of a nitro group into the benzylidene fragment leads to conformational changes in comparison to hydrazones **4** and **7**. For **6** (Fig. 1, **6**) as well as in the molecules of hydrazide **2** an $\mathbf{E}_{C(1)–C(2)}$-conformation [(torsion angle O(1)–C(1)–C(2)–O(2) is equal 176.6(3)°] is observed, instead of a $\mathbf{Z}_{C(1)–C(2)}$-conformation for hydrazones **4** and **7**. In molecule **6** the torsion of the *tert*-butylphenyl fragment around the C(3)–O(2) bond is essentially greater than in molecules **4** and **7** [(torsion angle C(2)–O(2)–C(3)–C(4) is equal to −45.3°(8)], but the deviation of the *tert*-butylphenoxy moiety from coplanarity with the hydrazone–amide fragment is much smaller (Table 3).

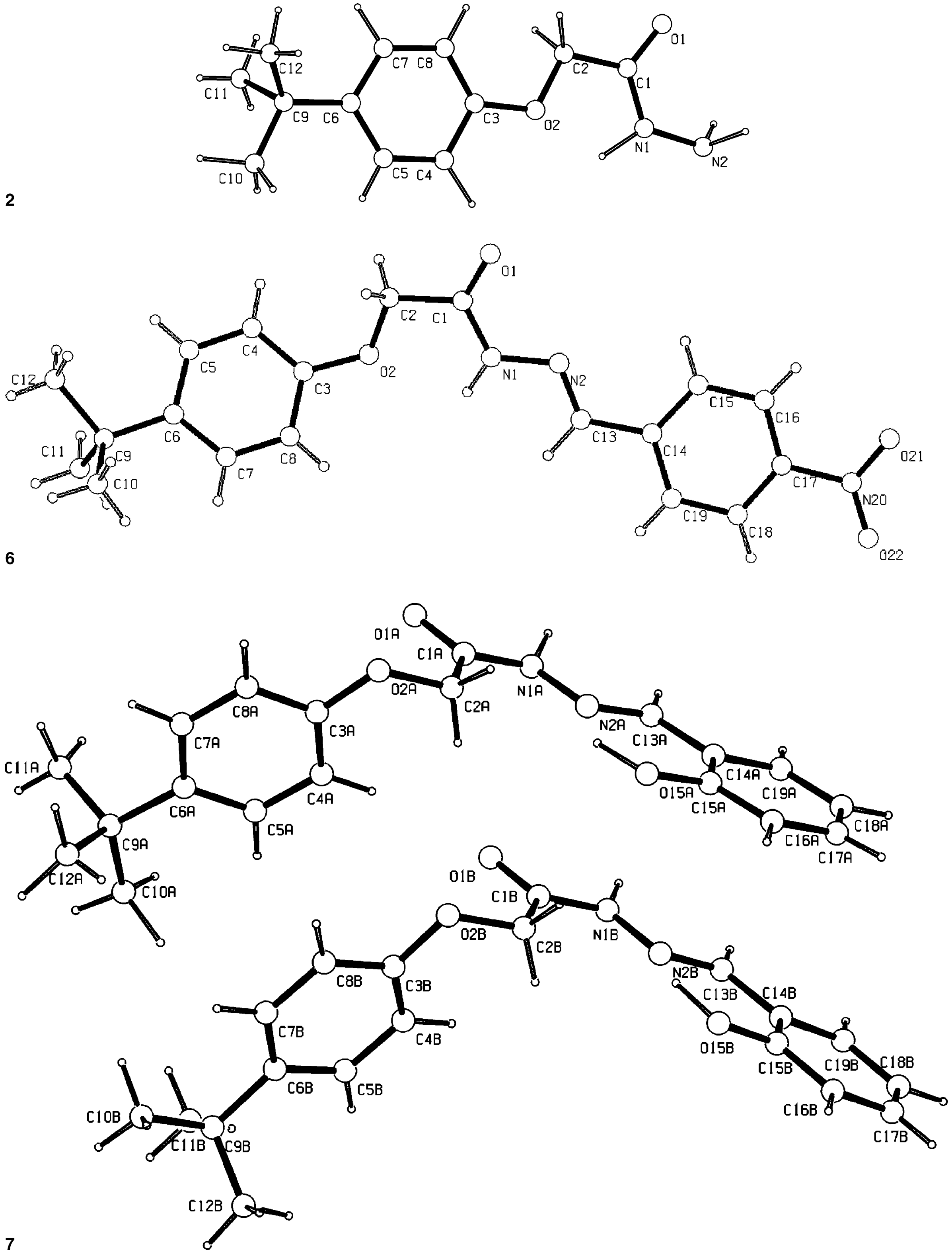

Fig. 1. Geometry of the molecules **2**, **6**, **7** and atomic numbering scheme (crystals **4** and **7** are isostructural).

Compared to hydrazones **4** and **7**, the phenyl ring of the arylideneimino fragment in hydrazone **6** is much more twisted (dihedral angles P2/P3 is equal 21.7(3)) relative to the optimal position for conjugation. Due to realization of the $\mathbf{Z}_{N\text{–}C(O)}$-conformation intramolecular NH···O hydrogen bonds between the amide and the ether (−OCH$_2$) groups in hydrazone are formed in spite of the fact that a pronounced turning of the 4-*tert*-butylphenyl fragment around the C(2)–O(2) and O(2)–C(3) bonds is observed. This intramolecular H-bond formed in the crystal by the amide group as in molecule **2** is complemented by an intermolecular H-bond with the C=O group of the adjacent molecule (Fig. 2, **6**).

The parameters of the H-bonds are the following: N(1)–H(1)···O(2), N–H 0.96 Å, H···O 2.16 Å, N(1)···O(2) 2.569(5) Å, angle N(1)–H(1)···O2 104°; N(1)–H(1)···O(1′) (1/2 + *x*, 1 − *y*, *z*): H···O 2.17, N(1)···O(1′) 3.079(5) Å, angle N(1)–H(1)···O(1′) 157°. A chain along the *X*-axis is formed via intermolecular H-bridges.

3.2. IR investigation

For investigation of conformational properties, intra- and intermolecular interactions depending on H-bonds the absorption bands of –NH, $-NH_2$ and –C=O groups in IR spectra are informative. To study such interactions IR spectra of compounds **2**–**9** were recorded in solid (polycrystalline) phase and in CCl_4 solution (Fig. 3).

The spectrum of hydrazide **2** in the solid state (Fig. 3, **2**) shows the $\nu_{as}(NH_2)$ as a shoulder (3340 cm^{-1}) on the strong peak at 3322 cm^{-1} and $\nu_s(NH_2)$ at 3205 cm^{-1}. The $\delta(NH_2)$ absorption forms a shoulder at ~1650 cm^{-1} on the ν(C=O) (1660 cm^{-1}) absorption band. A strong peak at 3322 cm^{-1} belongs to ν(NH). This assignment results from the comparison of the relative intensities of ν(NH) in the spectra of compounds **3**–**9**, where only NH groups, but no NH_2 groups are present. It should be noted according to literature data $XC(O)NHNH_2$ group may give only two bands for free vibrations ν(NH) and $\nu(NH_2)$ in region 3500–3400 cm^{-1} [14,15]. The above-mentioned frequencies of these absorption bands of the hydrazide **2** in crystalline phase are significantly lowered. This indicates that they all belong to fragments involved in hydrogen bonding. The presence of absorption band with a maximum at ~1540 cm^{-1} (amide II band δ(NH)), which can be observed as a shoulder on the strong peak at 1518 cm^{-1} (ν(CC) phenyl group), is an indication on the $\mathbf{Z}_{N-C(O)}$-conformation of the amide NH group [15].

According to Bellamy–Williams correlation [15], the frequencies ν_{as} and ν_s of the NH_2 amine groups for "free" or equal N–H bonds follow Eq. (1):

$$\nu_s = 345.53 + 0.876\nu_{as} \tag{1}$$

Hence $\nu_s(NH_2)$ for the described solid state should be: $\nu_s = 345.53 + 0.876 \times 3340 = 3271$ cm^{-1}. We observed a band at 3205 cm^{-1}. It indicates that the NH_2 groups of the primary amine fragments take part in an asymmetric H-bonds, which is in agreement with the data from the X-ray analysis (Fig. 2, **2**).

When going to solution in CCl_4 the spectrum of hydrazide **2** in the selected areas of ν(NH), $\nu(NH_2)$ and ν(C = O) absorption changes pronouncedly (Fig. 3, **2**). All above-mentioned

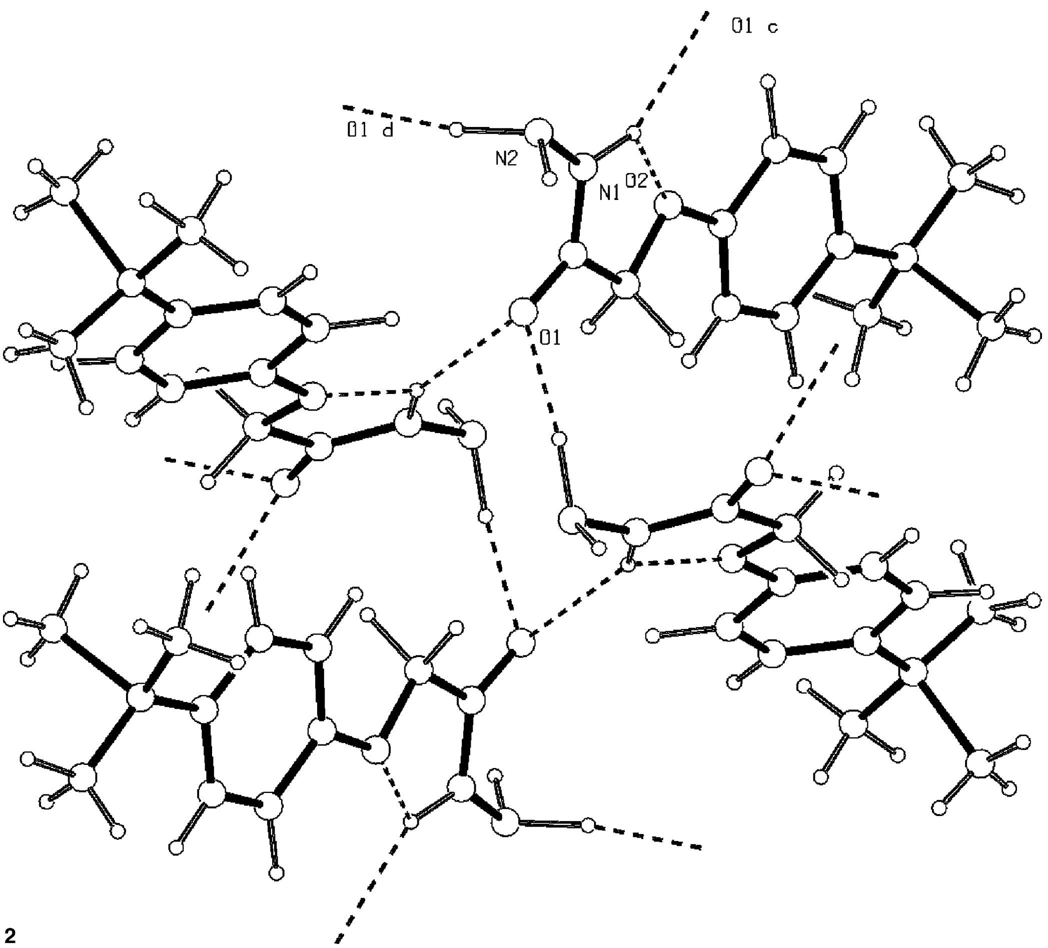

2

Fig. 2. Hydrogen bonds in the structures **2**, **6** and **7** (crystals **4** and **7** are isostructural).

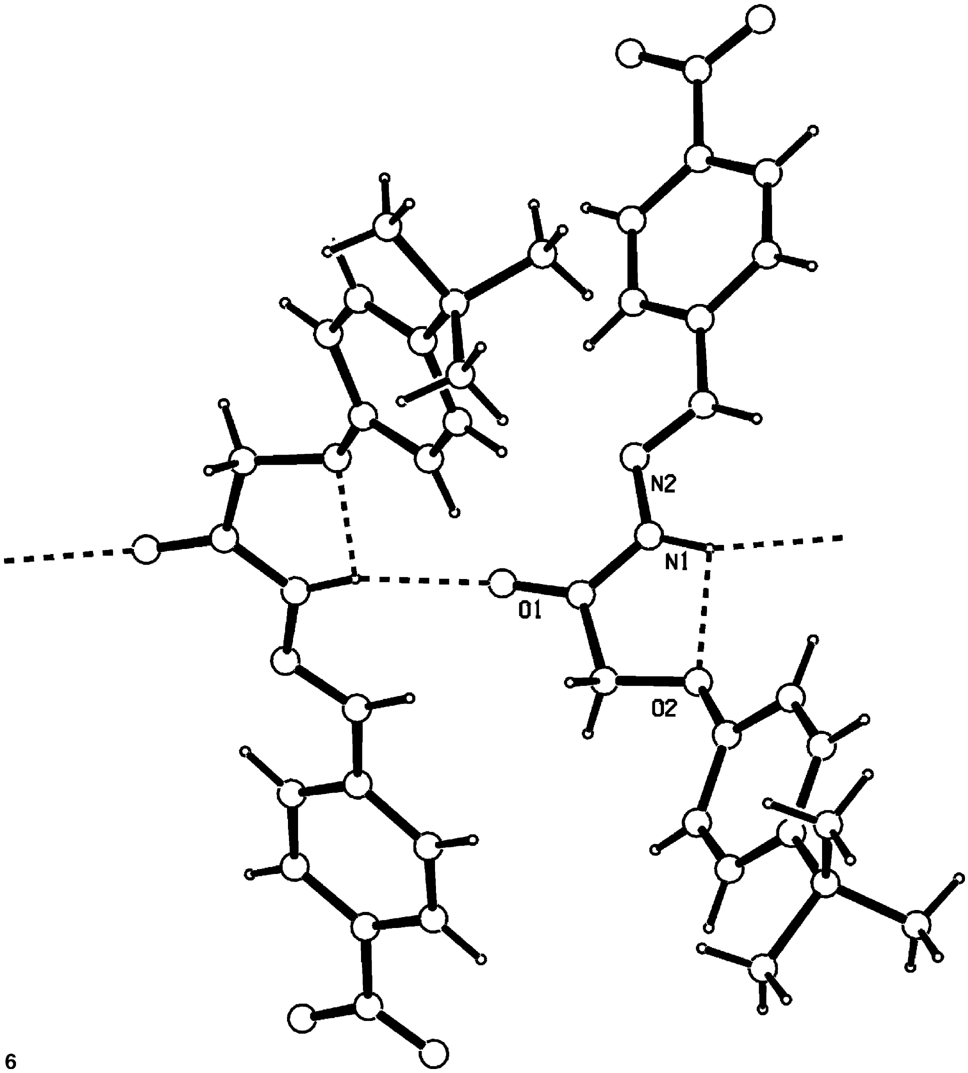

6

Fig. 2. (*Continued*)

absorption bands of associated NH_2 and NH practically disappear already at a concentration of $\sim 10^{-2}$ M. Instead of them a strong peak ν(NH) at 3452 cm^{-1} with a shoulder $\nu_{as}(NH_2)$ at ~3445 cm^{-1} and a weak peak $\nu_s(NH_2)$ at 3338 cm^{-1} with shoulders at 3367 and 3292 cm^{-1} can be observed. Hence all intermolecular bonds have been disrupted and, as follows from the observed bands in comparison to literature data [14], only non-associated molecules with possible intramolecular hydrogen bonds are present. In agreement with it, the frequency of the $\delta(NH_2)$ band decreased to 1627 cm^{-1} and ν(C=O) increased to 1693 cm^{-1}.

According to Bellamy–Williams Eq. (1) free $\nu_s(NH_2)$ should be about 3363 cm^{-1}. Hence the shoulder at 3367 cm^{-1} can probably be assigned to those molecules, which are free of hydrogen bonds involving the $-NH_2$ group. The frequency of the peak 3338 cm^{-1} indicates the presence of an intramolecular hydrogen bond of the NH_2 group with any proton acceptor in the non-associated molecules in this case. Another shoulder at 3292 cm^{-1} disappears during dilution and most probably corresponds to the short chain block of the associates bound by intermolecular hydrogen bonds.

It is necessary to note again that the presence of the peak δ(NH) at ~1540 cm^{-1} in the solid phase and 1545 cm^{-1} in solution indicates the $\mathbf{Z}_{N\text{–}C(O)}$-form of the amide fragment. The comparison of the value of the ν(NH) frequency 3322 cm^{-1} in solid phase and 3452 cm^{-1} in CCl_4 solution with literature data [14] also shows that hydrazide **2** in crystalline form and in CCl_4 solution exists only in $\mathbf{Z}_{N\text{–}C(O)}$-conformation. The presence of a single conformer in solution is also confirmed by a characteristic singlet peak ν(C=O).

In acylhydrazones of acetone NH_2 group is absent and a non-equivalent isomerization around C=N double bond is excluded. The region of NH stretching vibrations in the IR spectra is simplified, but those of carbonyl absorptions (1692 cm^{-1}) in solid get more complicated due to the ν(C=N) vibration (1646 cm^{-1}) (Fig. 3, **3**). The absorption peak δ(NH) at 1543 cm^{-1} is of analytical importance. The peak is a characteristic for the $\mathbf{Z}_{N\text{–}C(O)}$-conformer of the amide fragment. At the same time ν(NH) absorption band is double and has maxima at 3245 and 3222 cm^{-1}. The low value frequency is a characteristic for the $\mathbf{E}_{N\text{–}C(O)}$-configuration of the amide group in H-cyclodimers [15,16]. So it can be concluded that hydrazone **3**

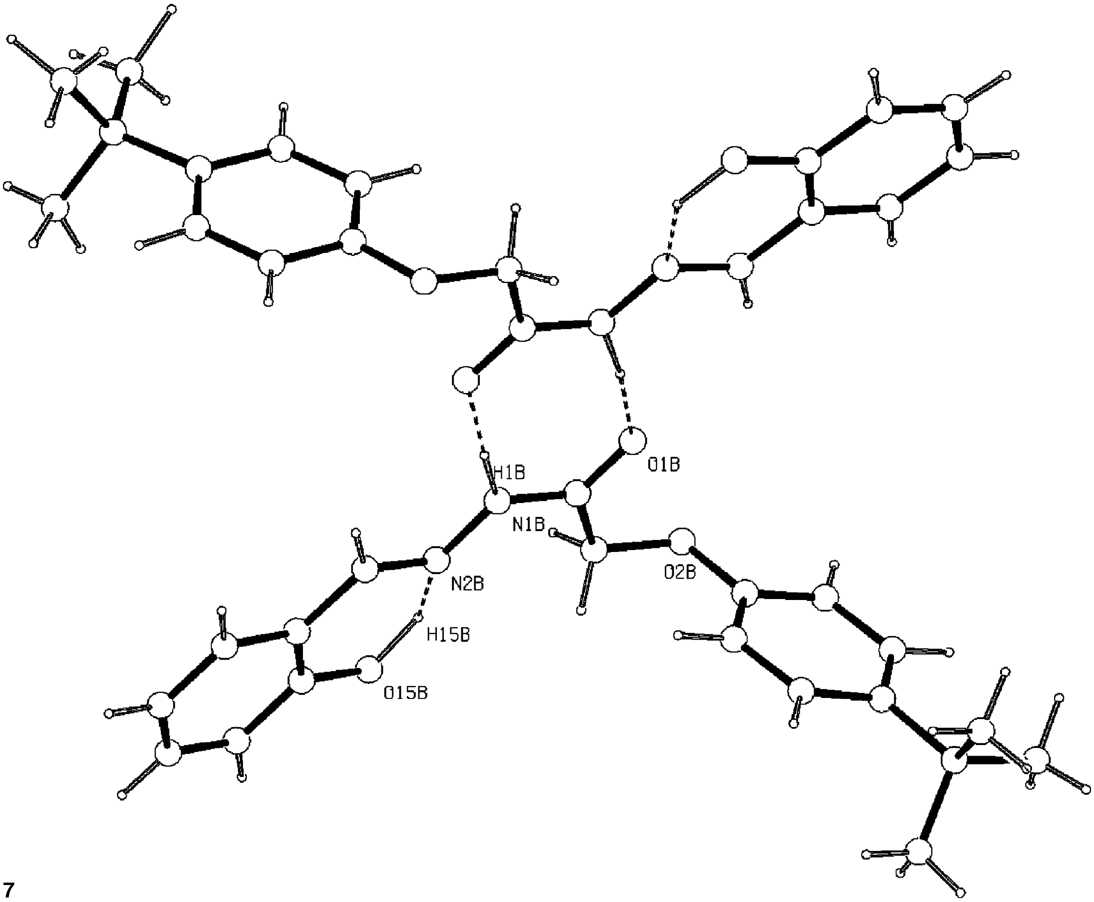

7

Fig. 2. (*Continued*).

in the solid state, according to the ratio of intensities of the doublet 3245 cm^{-1}/3222 cm^{-1}, consists of a mixture of about equal parts of H-bridged dimers of $\mathbf{E}_{N–C(O)}$-conformers and of intermolecularly bonded $\mathbf{Z}_{N–C(O)}$-conformers.

In contrast to the case of **2**, the ν(NH) vibration bands of the intermolecular hydrogen bonds remain but shift to 3195 cm^{-1} as the hydrazone **3** concentration in CCl_4 is decreased from 10^{-2} to 10^{-3} M (Fig. 3, **3**). The vibration bands disappear only at 10^{-4} M. This value of frequency is typical for the $\mathbf{E}_{N–C(O)}$-conformers of amides and is in agreement with literature data about stronger intermolecular hydrogen bonds formed by the $\mathbf{E}_{N–C(O)}$-conformers in comparison with the $\mathbf{Z}_{N–C(O)}$-conformers of secondary amides [15]. The fact that the band with a maximum at 3195 cm^{-1} does not shift to higher frequencies during dilution is typical for cyclic H-dimers of the $\mathbf{E}_{N–C(O)}$-conformers, which are not bound via additional intermolecular H-bonds [16]. The concentration decrease of **3** is also accompanied by the appearance of weak peaks of multiplet in region ~3400 cm^{-1}. Considering their relative intensities, the peaks have to be assigned in the following way: 3413 and 3452 cm^{-1}—ν(NH) vibrations of monomers of the $\mathbf{Z}_{N–C(O)}$-conformers with and without intramolecular NH···O hydrogen bonds between the amide and the ether group respectively, 3391 cm^{-1}—monomers of the $\mathbf{E}_{N–C(O)}$-conformer, band at 3359 cm^{-1}—overtone of the carbonyl absorption. The carbonyl peak at 1713 cm^{-1} grows, and the peak at 1697 cm^{-1} shrinks during dilution, being outstripped in intensity by the former peak. For this reason the first one has to be assigned to $\mathbf{Z}_{N–C(O)}$- and the second to the $\mathbf{E}_{N–C(O)}$-conformer and their associates.

Thus the hydrazone of acetone **3** in the solid state exists as a mixture of equal parts of the $\mathbf{E}_{N–C(O)}$- and $\mathbf{Z}_{N–C(O)}$-conformers. However in solution as the dilution increases, the $\mathbf{Z}_{N–C(O)}$-form becomes slightly dominant.

For acetylhydrazones of aromatic aldehydes in crystal and solution of different polarity only one $\mathbf{E}_{C=N}$-isomer is usually realized [5,6,17], which is in agreement with the X-ray data for **4**, **6**, **7**. It should be noticed that the spectral behaviour of aldehyde hydrazones **4**, **5**, **7** is similar in contrast to the behaviour of hydrazones **6**, **8**, **9**. Therefore the spectra of the benzylidene derivative **4** and some spectral peculiarities of compounds **6**, **8**, **9** have been investigated in more detail.

X-ray analysis of the monocrystal of hydrazone **4** showed that the molecules of this compound exist as H-cyclo-dimers of the $\mathbf{E}_{N–C(O)}$-conformers. In the IR spectra of **4** in solid state a peak with a maximum at 3193 cm^{-1} can be clearly observed (Fig. 3, **4**) which is caused by intermolecular hydrogen bonds in the $\mathbf{E}_{N–C(O)}$ cyclo-H-dimer. There are some striking peculiarities of the IR spectra in the range of N–H stretching vibrations. More longwave and intensive additional absorption at ~3090 cm^{-1} was registered along with the $\mathbf{E}_{N–C(O)}$ peak at ~3195 cm^{-1} in spectra of arylaldehyde hydrazones **4**, **5**, **7**, **8**. For **9** the

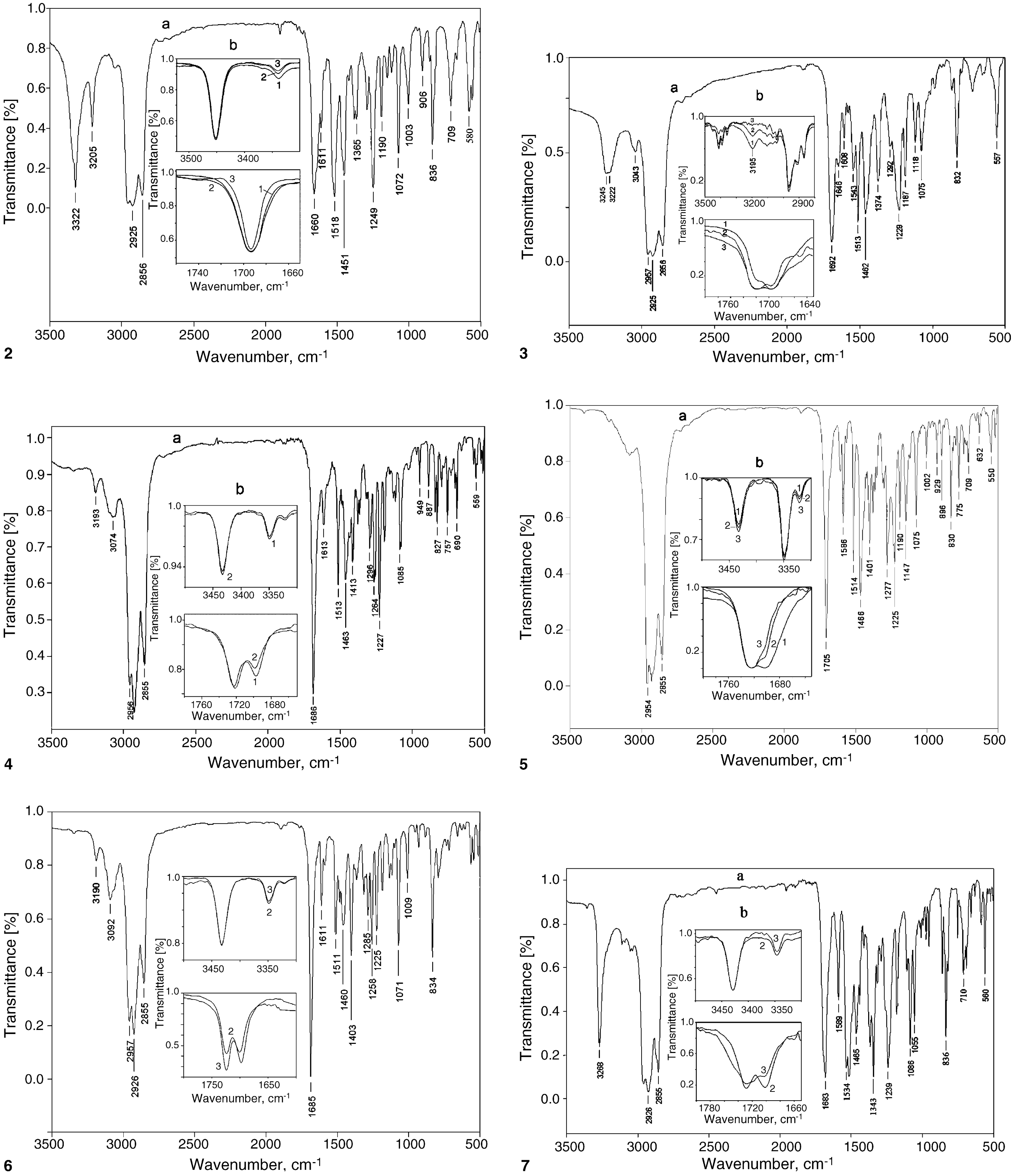

Fig. 3. IR spectra of compounds **2-9** (a) in nujol and (b) in CCl_4 at concentrations: (1) 10^{-2} M; (2) 10^{-3} M; (3) 10^{-4} M. For the solutions only the regions of ν(NH), ν(C=O) are shown.

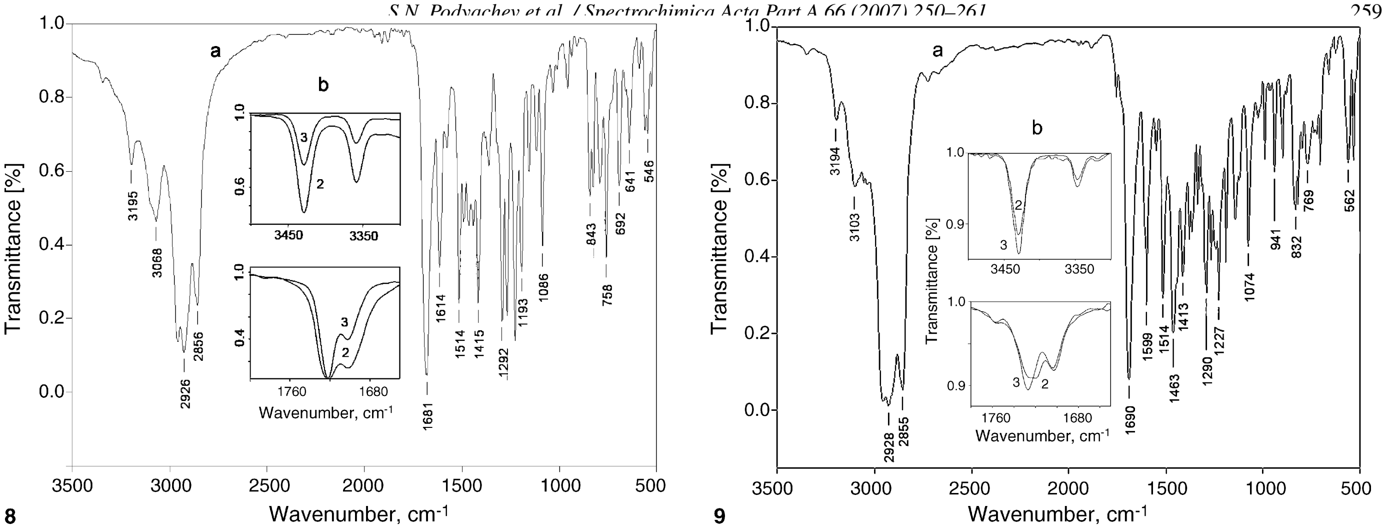

8

9

Fig. 3. (*Continued*).

peak at ~3090 cm^{-1} is only observed. In spectra of hydrazones **6** vice versa—the high-frequency peak at 3268 cm^{-1} is more intensive than low-frequency peak at ~3090 cm^{-1}. According to literature data, it is due to Fermi resonance between ν(NH) vibration and overtone – 2δ(NH) of $\mathbf{Z}_{\text{N-C(O)}}$-conformer or composite tone - ν(C=O) + δ(NH) of $\mathbf{E}_{\text{N–C(O)}}$-conformer. However, the corresponding absorption of secondary amides as a rule is much weaker than the main absorption in region above ~3200 cm^{-1} [15]. The observed reverse phenomenon for our compounds obviously results from the aromatic character of imine group substituents in discussed row. In fact the range of 3000–3100 cm^{-1} is a characteristic for unsaturated (aromatic and similar ones) ν(=CH) vibrations. The resonance effect complicated by their participation leads obviously to anomalous absorption of stretching vibrations at ~3090 cm^{-1} for $\mathbf{E}_{\text{N–C(O)}}$-conformers in the solid state. It may be an important diagnostic criterion for these conformers. The ν(NH) main band of $\mathbf{Z}_{\text{N–C(O)}}$-forms is replaced at higher frequencies region than for $\mathbf{E}_{\text{N–C(O)}}$-forms and usually doesn't give such effect. That is observed in the case of hydrazone **6**.

In the solutions of hydrazone **4** at concentrations below 10^{-3} M the absorption of the cyclo-H-dimers is not observed. The peak ν(NH) at 3433 cm^{-1}, which appears when going from the solid state to solution and which dominates among others in this region, represents the $\mathbf{Z}_{\text{N–C(O)}}$-form. The peak of its partner at 3349 cm^{-1}, can be assigned to the $\mathbf{E}_{\text{N–C(O)}}$-conformer. The intensity of the low-frequency component of doublet ν(C=O) (1723 and 1697 cm^{-1}) decreases under dilution, accompanied by a slightly decreasing of the intensity of peak 3349 cm^{-1}. This is probably the case of overlapping this latter with overtone –2ν(C=O). The peaks for ν(C=O), as in the case of hydrazone **3**, have to be assigned to the $\mathbf{Z}_{\text{N–C(O)}}$-at 1723 cm^{-1} and to the $\mathbf{E}_{\text{N–C(O)}}$-conformer together with associates forms at 1697 cm^{-1}, respectively. The relative low frequency of the peak ν(NH) for the $\mathbf{E}_{\text{N–C(O)}}$-conformer at 3349 cm^{-1} can be caused by the presence of long chain conjugation in the molecule. The same conclusions can be also drawn from IR spectra of 4-bromo- and 2-hydroxyphenylhydrazones **5**, **7** (Fig. 3, **5**, **7**).

For hydrazone **6**, which contains a nitro group in the benzylidene fragment a rather strong main absorption peak at 3268 cm^{-1} with a shoulder at ~3200 cm^{-1} in the ν(NH) region of polycrystalline phase is observed (Fig. 3, **6**). The frequency of this peak for **6** in comparison with compounds **4**, **5**, **7** is much higher. Obviously it is caused by the $\mathbf{Z}_{\text{N-C(O)}}$-form of the molecule, in which the hydrogen atom of the NH group according to X-ray data is connected by bifurcated H-bonds (Fig. 2, **6**). The shoulder at ~3200 cm^{-1} may indicate the presence of H-cyclodimers of the $\mathbf{E}_{\text{N–C(O)}}$-conformers in polycrystalline state. However it is also reasonable that the combination- and overtones in the region ~3200 cm^{-1} can be observed. Since X-ray analysis of the monocrystal **6** showed only $\mathbf{Z}_{\text{N–C(O)}}$-conformer.

The above-mentioned ν(NH) peaks for solid state **6** disappear and new ones (a major peak at 3429 cm^{-1}, belonging to the $\mathbf{Z}_{\text{N–C(O)}}$-form, and a second at 3346 cm^{-1} for the $\mathbf{E}_{\text{N–C(O)}}$-form) appear when going to CCl_4 solution. At the same time the band for ν(C=O) splits into peaks at 1728 and 1702 cm^{-1} with increasing relative intensity of the first peak during dilution. The peak at 1728 cm^{-1} obviously belongs to $\mathbf{Z}_{\text{N–C(O)}}$-conformers of the free molecules, the another – to $\mathbf{E}_{\text{N–C(O)}}$- and associated forms. The δ(NH) absorption can hardly be used for an investigation because of overlapping with the region of the very strong $\nu_{\text{as}}(NO_2)$ absorption at ~1520 cm^{-1} and $\nu_{\text{s}}(NO_2)$ at 1343 cm^{-1} (Fig. 3, **6**).

The, presence of an *ortho*-hydroxy substituent in the phenyl ring of the salicylidene hydrazone **7** is responsible for the broad dome-shaped ν(OH) band in the IR spectrum of the crystal **7**. This band is underneath the ν(NH), ν(=CH), ν(−CH) absorptions in the region ~3300–2800 cm^{-1} with a center at around ~3100 cm^{-1}. The other bands typical for ν(OH) vibrations and usually observed in the region 3200–3650 cm^{-1} [15] have not been registered. In CCl_4 solutions the broad dome-shaped ν(OH) band remains. This means that the hydrogen atom of the *ortho*-hydroxy group forms very strong intramolecular hydrogen bonds with sp^2-hybridized free electron pair of the nitrogen atom of the azomethine group ($\Delta\nu$ = 3610–3050 cm^{-1} = 560 cm^{-1}) that was clearly recognized by X-ray analysis The rule of

Johannsen (Eq. (2)) [18] was applied for the determination of this intramolecular hydrogen bond energy:

$$(\Delta H)^2 = 1.92[(\Delta \nu) - 40]\,\mathrm{kJ\,mol^{-1}} \qquad (2)$$

For intramolecular hydrogen bonds OH···N=C in hydrazone **7** the $-\Delta H$ calculated ~30 kJ mol^{-1}.

The hydrazone **8** containing 4-pyridine fragment shows in solid state a spectral similarity with the phenyl analogue **4**. It concerns the fragments NH and C=O (Fig. 3, **8**). In the region of ν(NH) vibrations for compound **8**, as well as for hydrazone **4**, a peak at 3194 cm^{-1} of the cyclic H-dimers of $\mathbf{E}_{\text{N–C(O)}}$-conformers is observed. However, in contrast to **4** the probable amide II peak δ(CNH) = 1549 cm^{-1} of the $\mathbf{Z}_{\text{N–C(O)}}$-conformation of the secondary amide structure also has to be mentioned. At the same time, ν(NH) peaks in the region ~3300 cm^{-1} for the $\mathbf{Z}_{\text{N–C(O)}}$-amide structure, which were observed for compounds **2** and **3** in the solid state, have not been registered for **8**. However in hydrazone **8** an absorption in the region at ~3100 cm^{-1} is observed. Probably, the $\mathbf{Z}_{\text{N–C(O)}}$-conformer of compound **8** in the solid state along with the usual intermolecular hydrogen bond forms also hydrogen bonds with the N-atom of the pyridine fragment of the molecule. The N-atom of the pyridine fragment is known as one of the strongest proton acceptors [15]. This probably leads to an additional shift ν(NH) to lower frequencies (~3100 cm^{-1}) for the $\mathbf{Z}_{\text{N–C(O)}}$-conformer and the enhancement of Fermi resonance with 2δ(NH).

This conclusion is confirmed by spectra in CCl_4 solution. Therein the intensity of the peak at 3103 cm^{-1} is step-by-step decreased with dilution and, as in **4**, a ν^{free}(NH) doublet appears: one peak at 3430 cm^{-1} assigned to the $\mathbf{Z}_{\text{N–C(O)}}$-conformer (more intense for diluted solution) and another one at 3347 cm^{-1} assigned to the $\mathbf{E}_{\text{N–C(O)}}$-conformer. Additionally also a doublet for ν(C=O) at 1720 cm^{-1}/1703 cm^{-1} appears. In more concentrated solution a small peak of the cyclic H-dimer with a maximum at 3211 cm^{-1} can be noted.

Unexpectedly, for hydrazone **9**, containing 2-pyridine fragment, only one absorption band with a maximum at 3084 cm^{-1} in solid is observed in the region of ν(NH) in contrast to **2–8** (Fig. 3, **9**). This band is broadened, as it usually happens for hydrogen bonded XH groups, and, as in the previous case for compound **4**, **5**, **7** and **8**, it overlaps with the aromatic ν(=CH) absorption but to a greater degree. The additional peaks in the region of ~1550 cm^{-1}, which could be assigned to δ(NH) in the $\mathbf{Z}_{\text{N-C(O)}}$-structure, cannot be observed except for νPh and νPy (1606, 1586 and 1564 cm^{-1}). The peak of ν(C=O) has maximum at 1705 cm^{-1} and is symmetric. Therefore one can suppose that the pyridine acceptor dominates in the NH proton bonding in hydrazone **9**. The lower frequency absorption bands of the multiple bonds of the pyridine fragments—1598 cm^{-1} (**8**) and 1586 cm^{-1} (**9**) also support this statement. It can be clearly seen that $\mathbf{E}_{\text{N–C(O)}}$-conformers form cyclic H-dimers, in which the NH groups are involved in probably bifurcated H-bonds with participation of the nitrogen atom of the pyridine fragments.

In CCl_4 solution of hydrazone **9** the absorption in the region of 3084 cm^{-1} gradually decreases; a weak band of ν(NH) with a maximum at 3215 cm^{-1} for the cyclic H-dimer of the $\mathbf{E}_{\text{N–C(O)}}$-conformer disappears upon dilution. So the IR spectrum becomes simpler. At the same time the sharp peaks at 3349 and 3433 cm^{-1} for ν^{free}(NH) of the $\mathbf{E}_{\text{N–C(O)}}$- and $\mathbf{Z}_{\text{N–C(O)}}$-form, respectively, are increasing. The ratio of the peak intensities of the conformers in contrast to the previous cases for **2–8** is inverse, namely the $\mathbf{E}_{\text{N–C(O)}}$-conformer dominates. As in the case of spectra **8** in CCl_4, a doublet ν(C=O) at 1724 cm^{-1}/1703 cm^{-1} appears and its lower frequency component is decreasing upon dilution. Consequently compound **9** in crystal phase exists as an $\mathbf{E}_{\text{N–C(O)}}$-conformer with very strong hydrogen bonds. There is an equilibrium of both amide structures with a predominance of the $\mathbf{E}_{\text{N–C(O)}}$-form in solutions of **9** probably due to some electronic effects of 2-pyridine fragment.

Following the *Johannsen* Eq. (2), the energy of intermolecular hydrogen bond in the cyclic H-dimers of $\mathbf{E}_{\text{N–C(O)}}$-form of investigated compounds can be approximately estimated to be equal: $(\Delta H)^2 = 1.92[(3350 - 3200) - 40]$; $-\Delta H \approx 14.5$ kJ mol^{-1}. Thus the whole energy of intermolecular hydrogen bonds in the cyclic H-dimer can be determined as 14.5 × 2 = 29 kJ mol^{-1}. The average energy of the H-bond in intermolecularly bonded associates of $\mathbf{Z}_{\text{N–C(O)}}$-conformers for **3** and **6** is obtained from the expression: $(\Delta H)^2 \approx 1.92[(3421 - 3245) - 40]$; $-\Delta H \approx 16.1$ kJ mol^{-1}.

One can roughly estimate the share of the $\mathbf{Z}_{\text{N–C(O)}}$- and $\mathbf{E}_{\text{N–C(O)}}$-forms in solution by the intensity ratio of the ν(NH) absorption bands. Thus, the ratio of $\mathbf{Z}_{\text{N–C(O)}}/\mathbf{E}_{\text{N–C(O)}}$ at a concentration of ≈10^{-4} M was determined as follows: hydrazide **2**–100/0%; **3** – 66%/34%; **4** – 69/31%; **5** – 63/37%; **6** – 78/22%; **7** – 64/36%; **8** – 75/25%; **9** – 40/60%.

4. Conclusion

A new series of 4-*tert*-butylphenoxyacetylhydrazones has been synthesized by reaction of 4-*tert*-butylphenoxyacetylhydrazide with aromatic aldehydes and acetone. Characteristic spectral parameters and structural peculiarities of the investigated molecules have been determined by means of X-ray analysis and IR spectroscopy. It was found that in solid state and CCl_4 solution 4-*tert*-butylphenoxyacetylhydrazide exists only as a $\mathbf{Z}_{\text{N–C(O)}}$-conformer. However its hydrazone derivatives in solid state exist as $\mathbf{E}_{\text{N–C(O)}}$ or $\mathbf{Z}_{\text{N–C(O)}}$-form as well as a mixture of these conformers. The $\mathbf{E}_{\text{N–C(O)}}$-conformer of 4-*tert*-butylphenoxyacetylhydrazone of salicylic aldehyde has intramolecular H-bonds OH···N ($-\Delta H$ = ~30 kJ mol^{-1}), which do not hinder the formation of cyclic hydrogen bonded dimers. The $\mathbf{Z}_{\text{N–C(O)}}$-conformer of 4-*tert*-butylphenoxyacetylhydrazide and 4-*tert*-butylphenoxyacetylhydrazone of 4-nitrobenzaldehyde in solid state has an intramolecular hydrogen bond of the NH···O type between the amide hydrogen atom and the oxygen atom of the phenoxy group. The presence of this intramolecular bond is probably the reason for the predominance of the $\mathbf{Z}_{\text{N–C(O)}}$-conformers in dilute CCl_4 solution in almost all investigated hydrazones. The energy of the intermolecular hydrogen bond in the cyclic H-dimers of the $\mathbf{E}_{\text{N-C(O)}}$-conformers and associates of the $\mathbf{Z}_{\mathrm{N–C(O)}}$-conformers has been estimated as 14.5 and 16.1 kJ mol^{-1}, respectively.

The diagnostically important IR spectral criteria required for the conformational analysis of acethylhydrazones have been established.

Thus, the nature of the substituent in the acetylhydrazone fragment of the molecules determines the character of hydrogen bonds, the conformational properties and characteristic spectral parameters of the investigated hydrazones.

Acknowledgements

This work was supported by the Russian Fund for Basic Research (grants 04-03-32992a, 04-03-32156aofi_a, 04-03-32156a) and a grant of the Academy of Science of the Republic of Tatarstan (07-7.1-264).

References

[1] E. Schmidt, Hydrazine and its Derivatives: Preparation, Properties, Applications, second ed., Wiley, New York, 2001.
[2] P.V. Bernhardt, P. Chin, D.R. Richardson, J. Biol. Inorg. Chem. 6 (2001) 801.
[3] V. Kogan, V. Zelentsov, G. Larin, V. Lhukov, Complexes of Transitional Metals with Hydrazones, Nauka, Moscow, 1990.
[4] U. Ragnarsson, Chem. Soc. Rev. 30 (2001) 205.
[5] G. Palla, G. Fredieri, P. Domiano, Tetrahedron 42 (1986) 3649.
[6] U. Himmerlreich, F. Tschwatschal, R. Borsdorf, Monatsh. Chem. 124 (1993) 1041.
[7] E.A. Alekseeva, V.A. Bacherikov, A.I. Gren, A.V. Mazepa, V.Y. Gorbatyuk, S.P. Krasnoshchekaya, Russ. J. Org. Chem. 36 (2000) 1321.
[8] S.N. Podyachev, B.I. Buzykin, D.V. Osyanina, V.V. Syakaev, S.N. Sudakova, I.A. Litvinov, R.R. Shagidullin, L.V. Avvakumova, W.D. Habicher, A.I. Konovalov, X International Seminar on Inclusion Compounds Book of Abstract, Kazan, Russia, 2005, p. 132.
[9] A. Yamada, T. Murase, K. Kikukawa, T. Arimura, S. Shinkai, J. Chem. Soc. Perkin Trans. 2 5 (1991) 793.
[10] S.S. Tiwari, A.K. Sen Gupta, K. Jaswant, J. Indian Chem. Soc. 51 (1974) 402.
[11] L.H. Straver, A.J. Schierbeek, MOLEN. Structure Determination System. Program Description, Nonius B.V., Delft, 1994. V. 1.
[12] G.M. Sheldrick, SHELX-97 (Release 97-2). Programs for Crystal Structure Analysis, University of Göttingen, Germany, 1997.
[13] A.L. Spek, Acta Cryst. (A) 46 (1990) 34.
[14] E. Titov, A. Grekov, I. Rybachenkov, V. Shevchenko, Teor. Eksp. Khim. 4 (1968) 742.
[15] L.J. Bellamy, The IR Spectra of Complex Organic Molecules, second ed., Methuen/Wiley, London/New York, 1958.
[16] N.B. Colthup, L.H. Daly, S.E. Wiberley, Introduction to Infrared and Raman Spectroscopy, Academic Press, New York/London, 1964.
[17] Yu.P. Kitaev, B.I. Buzykin, Hydrazones, Nauka, Moscow, 1974.
[18] A.V. Iogansen, Spectrochim. Acta Part A 55 (1999) 1585.